Vortex-Lattice Phase Transitions in $Bi_2Sr_2CaCu_2O_8$ Crystals with Different Oxygen Stoichiometry

B. Khaykovich,[1] E. Zeldov,[1] D. Majer,[1] T. W. Li,[2] P. H. Kes,[2] and M. Konczykowski[3]
[1]*Department of Condensed Matter Physics, The Weizmann Institute of Science, 76100 Rehovot, Israel*
[2]*Kamerlingh Onnes Laboratorium, Rijksuniversiteit Leiden, P.O. Box 9506, 2300 RA Leiden, The Netherlands*
[3]*CNRS, URA 1380, Laboratoire des Solides Irradiés, École Polytéchnique, 91128 Palaiseau, France*
(Received 31 August 1995)

The vortex-lattice phase transitions in $Bi_2Sr_2CaCu_2O_8$ crystals with various oxygen stoichiometry are studied using local magnetization measurements. Three new findings are reported: The first-order phase transition line at elevated temperatures shifts upward for more isotropic overdoped samples. At lower temperatures another sharp transition is observed that results in enhanced bulk pinning in the second magnetization peak region. The two lines merge at a multicritical point at intermediate temperatures forming apparently a continuous phase transition line that is anisotropy dependent.

PACS numbers: 74.60.Ec, 74.60.Ge, 74.60.Jg, 74.72.Hs

The mixed state of high-temperature superconductors (HTSC) has a very complicated phase diagram. The nature of the different vortex phases and the thermodynamic transitions between them are of fundamental interest, and are the subject of substantial recent theoretical and experimental efforts [1–10]. It is generally accepted that the high anisotropy plays a crucial role in the richness of the phase diagram of HTSC. Nevertheless, a systematic study of the anisotropy effects is quite complicated and was limited so far by the lack of a well defined phase boundary that could be monitored as a function of the anisotropy. A recent advance in local measurements has revealed a sharp step in magnetization due to a first-order vortex-lattice phase transition in $Bi_2Sr_2CaCu_2O_8$ (BSCCO) crystals [10]. Such a clearly defined fundamental transition is thus a natural candidate for an investigation of the anisotropy effects in HTSC, and this paper presents a first study in this direction. Another intriguing feature of the phase diagram of many HTSC crystals, and BSCCO in particular, is the anomalous second magnetization peak at lower temperatures. The associated increase of magnetization with magnetic field has been attributed to surface barrier effects [11], crossover from surface barrier to bulk pinning [12], sample inhomogeneities [13], dynamic effects [14], and 3D to 2D transitions [15–17]. Our local measurements indicate that a very abrupt upturn in the bulk critical current occurs at the onset of the second peak in BSCCO. We postulate that this behavior is triggered by an underlying thermodynamic phase transition of the flux-line lattice. Furthermore, for the different anisotropy crystals the two phase transition lines are found to form, apparently, one continuous transition line that changes from first to possibly second order at a critical point. The existence of such a phase transition at low temperatures at flux densities on the order of H_{c1} is unprecedented and calls for new theoretical and experimental studies.

The BSCCO crystals were grown by the traveling solvent floating zone technique [18,19]. The experiments were carried out on several as-grown crystals [18,19] with typical dimensions of $700 \times 300 \times 10\ \mu m^3$ and on two crystals [19] which were heat treated in order to change the oxygen stoichiometry [20]. The as-grown crystals from both sources show practically identical phase diagrams. The overdoped crystal (annealed at 500 °C in air) with $T_c \simeq 83.5$ K was cut to $620 \times 180 \times 40\ \mu m^3$ and the optimally doped crystal (annealed at 800 °C) with $T_c \simeq 89$ K to $600 \times 300 \times 15\ \mu m^3$. As shown in [20], annealing in air between 500 and 800 °C reversibly changes the oxygen stoichiometry. With increasing oxygen content both the c axis and T_c decrease linearly with the oxygen concentration. In addition, the in-plane penetration depth $\lambda(0)$ decreases, from 240 to 260 nm for the optimally doped to 180 nm for the overdoped sample [21]. This change of $\lambda(0)$ with oxygen content is also seen in ceramic BSCCO samples [22] and reflects the increase in hole concentration with overdoping. It was further shown [23] that the ratio between the c-axis and ab-plane resistivities at 100 K also depends strongly on the oxygen contents. Both studies report a reduction of ρ_c/ρ_{ab} by a factor of about 3 when going from optimally to strongly overdoped. These results strongly suggest that the small anisotropy ratio ε in the superconducting state also depends on the oxygen stoichiometry with overdoped samples being more isotropic. In addition, oxygen content influences the value of the critical current at low temperatures and high fields [21]. However, in the higher temperature and low field region that is of interest here, no observable change in pinning was obtained. The as-grown crystals from both sources have doping levels close to optimal ($T_c \simeq 90$ K), but the exact oxygen stoichiometry is not known due to the vertical growth process which is very slow, about 0.2 mm/h. The already crystalline part is thus annealed at temperatures ranging between the melting temperature (860 °C) and the water-cooled clamp, and is dictated by the vertical temperature gradient in the air atmosphere and the thermal conductivity of the boule.

 © 1996 The American Physical Society

The local magnetization measurements were performed in applied field $H_a||z||c$ axis using arrays of 10×10 μm^2 GaAs/AlGaAs Hall sensors [24,25].

Figure 1 illustrates typical local magnetization loops as measured by the sensors. The first-order transition [10] is clearly seen as a small positive sharp step in $B_z - H_a$ at elevated temperatures as demonstrated for the as-grown crystal at 64 K [Fig. 1(a)] and for the overdoped crystal at 70 K [Fig. 1(b)]. Figure 2 shows the mapping of the first-order transition as a function of temperature for three crystals of different oxygen stoichiometry, i.e., different anisotropy. We find that the transition line shifts significantly with anisotropy and moves to higher fields for more isotropic crystals. In addition, in all the crystals the first-order transition terminates abruptly at a sample dependent critical point (indicated by arrows) in the range of 40 to 50 K [10]. Two scenarios have been proposed for the first-order phase transition, the melting of the vortex lattice [5] and the decoupling of the vortex-line liquid into uncorrelated vortex pancakes [4]. In both cases, the predicted transition line is very sensitive to anisotropy ε [1], and scales as ε^2. Therefore, the observed anisotropy effect (Fig. 2) is consistent with both theories and does not resolve this ambiguity. The temperature dependence, however, should be different. According to the melting theory [5], an approximate power-law behavior $B_m(T) = B_0(1 - T/T_c)^\alpha$ is expected, where $\alpha \leq 2$. The best fit for the optimally doped crystal results in a high value of $\alpha \simeq 2.28$ and unrealistic $T_c \simeq 104$ K. As-grown crystals give $\alpha \simeq 1.57$, $T_c \simeq 94.6$ K, and the overdoped one results in $\alpha \simeq 1.51$ and $T_c \simeq 88$ K. The melting fits produce too high values of T_c for all the samples and a sample dependent α. Therefore we cannot derive a consistent estimate of ε from these fits. The decoupling scenario, on the other hand, results in much more consistent fits as shown by the solid lines in Fig. 2. The theory [4] predicts $B_D(T) = B_0(T_c - T)/T$, where $B_0 \approx \alpha_D \varepsilon^2 \phi_0^3/[4\pi\lambda(0)]^2 T_c d$. Here $\alpha_D \simeq 0.1$ is a universal parameter, and $d \simeq 15$ Å is the interlayer spacing that varies by less than 0.1 Å with changing the annealing temperature [17,20]. Note that this equation depends on the combination of ε and $\lambda(0)$. Since we know $\lambda(0)$ from [21], we are able to estimate the change in anisotropy due to variation in oxygen stoichiometry. The obtained values are $\varepsilon^{-1} \simeq 100$ for the overdoped sample (lower anisotropy), $\varepsilon^{-1} \simeq 120$ for the as-grown, and $\varepsilon^{-1} \simeq 130$ for the optimally doped (higher anisotropy). We conclude that the optimally doped sample has indeed the largest anisotropy. Currently, there is unfortunately no reliable method for a direct quantitative measurement of such high ε^{-1}. It is interesting to note that a recent analysis of the melting behavior in layered superconductors at low fields [6] predicts a power-law dependence of $B_m(T)$ with $\alpha = 1.5$ and B_0 that scales with ε/λ^3 rather than ε^2/λ^2. Also in this case, using the above estimates of λ, our data in Fig. 2 imply a similar relative variation of ε for the studied crystals. A simultaneous and independent determination of both ε and $\lambda(0)$ is therefore of major importance for determination of the origin of the observed first-order phase transition. Note also that neither melting nor decoupling theories account for the flattening of the transition line near the critical point and the critical point itself (see Fig. 2).

We now discuss the behavior at temperatures below the critical point. As demonstrated in Fig. 1(c), a large second magnetization peak is observed at fields above $B_{sp}(T)$. The magnetization changes abruptly at B_{sp} in opposite directions on increasing and decreasing fields in contrast to the behavior at B_m. Analysis of the field profiles across the sample shows a transition from smooth dome-shaped profiles due to surface and geometrical barriers at low fields to Bean profiles due to the onset

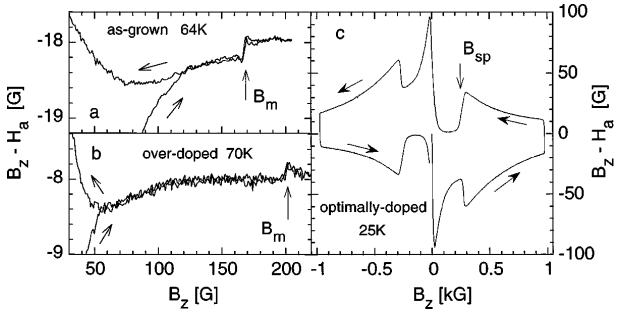

FIG. 1. Local magnetization loops $B_z - H_a$ measured in the central part of BSCCO crystals as a function of *local* magnetic induction. At elevated temperatures a first-order transition is manifested by equilibrium magnetization step at B_m presented for the as-grown crystal at $T = 64$ K (a) and overdoped crystal at $T = 70$ K (b). At low temperatures a sharp, possibly second-order, transition is observed at the onset of the second magnetization peak B_{sp} as shown for the optimally doped crystal at $T = 25$ K (c).

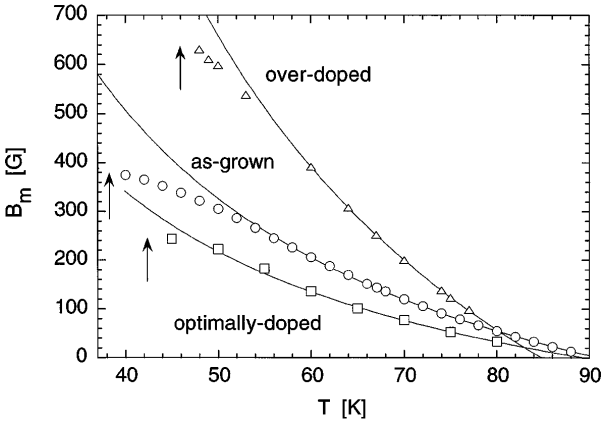

FIG. 2. The first-order phase transition $B_m(T)$ for three BSCCO crystals of different anisotropy. The solid lines are fits to the decoupling transition $B_m(T) = B_0(T_c - T)/T$ with $T_c \simeq 84.8$ K, $B_0 \simeq 946$ G for the overdoped sample (△), $T_c \simeq 91.0$ K and $B_0 \simeq 397$ G for as-grown (○), and $T_c \simeq 89.5$ K, $B_0 \simeq 275$ G for the optimally doped crystal (□). The arrows indicate the position of the critical point.

of significant critical currents at fields above B_{sp} [26]. Several models have been proposed to explain the origin of this enhancement of critical current based on pinning by oxygen-deficient regions [13], dynamic effects due to different relaxation rates in single-vortex and small-bundle pinning regimes [14], and the existence of a dimensional crossover field B_{2D} [15–17]. All these models describe crossover processes in which the width of the transition region is on the order of the characteristic field at the transition. It is important, therefore, to determine the width of the transition over which the critical current J_c is built up. In global measurements the observed onset of the second magnetization peak is broad [14,15] since the magnetization builds up gradually with H_a and reaches a maximum only when a fully penetrated new critical state is obtained. In addition, the global measurement averages over regions of different values of B, and therefore different values of $J_c(B)$, across the sample. The use of Hall sensors, on the other hand, lifts this limitation. In the Bean model [27] the field gradient dB_z/dx is a direct measure of J_c. In a platelet geometry the situation is more complicated [28], but, nevertheless, dB_z/dx remains proportional to J_c and hence can be used for a direct evaluation of the behavior of J_c. Figure 3(a) shows the experimental dB_z/dx in the second peak region on decreasing H_a, obtained by differentiating the field measured by adjacent sensors. dB_z/dx is seen to drop very sharply as H_a is decreased. This drop occurs at different values of H_a at various locations inside the crystal, starting from the edges and moving towards the center due to the nonuniform field profile $B_z(x)$. Figure 3(b) shows the same data plotted as a function of local B_z at each location. The striking observation of overlapping curves demonstrates that the sharp drop of local J_c occurs whenever the local field reaches $B_{sp}(T)$ regardless of the position. The width of the transition is about 5 G $\simeq$ 1.5% of B_{sp}. These measurements were specifically made by smaller sensors, of 3×3 μm^2 size, in order to demonstrate that the transition is *locally* very sharp. When measured by 10×10 μm^2 sensors, the observed width of the transition is about 20 G, indicating that the apparent width is limited by the sensor size. Therefore, the real width of the transition must be even narrower than in Fig. 3(b). We do not resolve a step in the local magnetization associated with a first-order transition. We therefore suggest that the sharp change in pinning at the onset of the second magnetization peak is driven by an underlying thermodynamic second-order phase transition with a width which is at least 2 orders of magnitude narrower than the characteristic field B_{sp}. We cannot exclude, though, that this is a weakly first-order transition with a magnetization step that is below our experimental resolution or obscured by the onset of bulk pinning. To the best of our knowledge, there is currently no theoretical explanation for the existence of a sharp vortex-lattice phase transition at low temperatures at such low fields on the order of H_{c1} [1].

Figure 4 shows the second peak line $B_{sp}(T)$ for three crystals along with $B_m(T)$. The position of B_{sp} is strongly anisotropy dependent [17] and shifts upwards for more isotropic samples. We find that this shift to higher fields is to the same extent as the shift of $B_m(T)$. Moreover, the first-order transition terminates at a temperature below which the second magnetization peak develops for each of the samples. $B_{sp}(T)$ and $B_m(T)$ merge at two sides of the same, sample dependent, critical point on the B-T phase diagram for the various anisotropies. This finding is a strong indication that the two lines represent, in fact, one continuous vortex-lattice transition that changes from first order to probably second order (or a weakly first order) at a tricritical point as the temperature is decreased. This interpretation is consistent with the fact that a first-order vortex-lattice phase transition is not expected to terminate

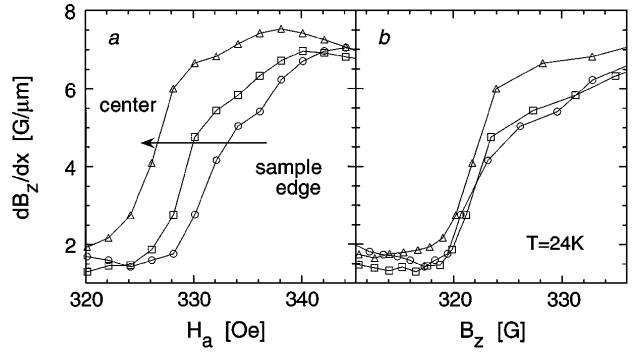

FIG. 3. Field gradients dB_z/dx as measured by three pairs of adjacent sensors 6 μm apart in the vicinity of the second magnetization peak on decreasing H_a in as-grown crystals. The transition at various locations occurs at different values of H_a (a), but at the same thermodynamic value of the local field B_z (b).

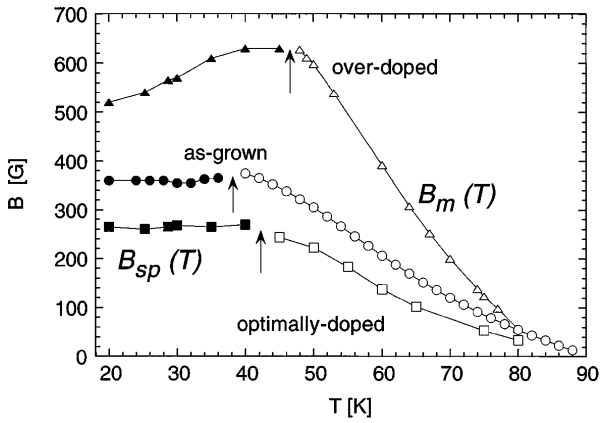

FIG. 4. First-order transition lines B_m (empty symbols) together with the second-order transition $B_{sp}(T)$ (filled symbols) for an overdoped sample with $T_c \simeq 83.5$ K (△), as-grown sample $T_c \simeq 90$ K (○), and optimally doped BSCCO crystal with $T_c \simeq 89$ K (□). $B_{sp}(T)$ was defined as the point of the steepest drop of the local magnetization peak on decreasing field as indicated by the arrow in Fig. 1(c). The arrows indicate the position of the critical point.

at a simple critical point and should be followed by a second-order phase transition due to involved symmetry breaking. The amplitude of the second magnetization peak decreases as the temperature is increased, and the peak becomes blurred and not very well defined close to the critical point, probably due to rapid relaxation of the bulk current at higher temperatures. This is the reason for the apparent gap in the data in a narrow temperature interval around the critical point (Fig. 4).

Above $B_m(T)$, the vortex lattice undergoes a transformation into some liquid phase with *reduced* vortex pinning. Above $B_{sp}(T)$, in contrast, a new phase with *enhanced* pinning is obtained. Two different phases at low and high temperatures must, therefore, exist above the entire phase transition line. One may thus anticipate the existence of another vertical phase transition or crossover line that separates the two high-field phases. The presence of such a vertical depinning line was recently reported [25]. This line shows no sharp features, but it seems to terminate at the same critical point as discussed above, which implies the existence of a multicritical point. A similar phase diagram was recently conjectured for $YBa_2Cu_3O_{7-\delta}$ (YBCO) crystals [8]. The presence of a multicritical point in YBCO at fields higher by more than 2 orders of magnitude is consistent with more than 1 order of magnitude lower anisotropy of YBCO as compared to BSCCO. The exact nature of the various vortex phases and the phase transitions in BSCCO is still unresolved. Taking into account that the neutron diffraction data [9] suggests an ordered Abrikosov lattice in the entire low-field phase, one possible scenario would be that $B_m(T)$ is a simultaneous melting and decoupling transition into a pancake liquid, whereas $B_{sp}(T)$ is a transition into a decoupled pancake solid. The high-field vertical transition would correspond to melting of the pancake solid. Such a phase diagram was recently proposed on the basis of Monte Carlo simulations [29], although it was concluded that in the absence of disorder the $B_{sp}(T)$ line is a smooth crossover rather than a sharp transition as reported here. Also, interestingly B_{sp} was predicted to show an upturn at low temperatures, whereas Fig. 4 indicates that $B_{sp}(T)$ has a tendency to decrease with decreasing T.

In conclusion, we find that a weakly pinned vortex lattice undergoes a sharp, probably second-order, phase transition into a strongly pinned state as the field is increased at low temperatures. At elevated temperatures, a first-order transition into an unpinned state is observed. The two lines seem to form one continuous phase transition of the vortex matter with a multicritical point at intermediate temperatures. This entire phase transition is significantly shifted to higher fields as the anisotropy of BSCCO crystals is reduced.

Discussions with V. B. Geshkenbein, V. M. Vinokur, A. I. Larkin, and G. Blatter are gratefully acknowledged. We are grateful to H. Motohira for providing the as-grown BSCCO crystals and to H. Shtrikman for growing the GaAs heterostructures. This work was supported by the Ministry of Science and the Arts, Israel, and the French Ministry of Research and Technology (AFIRST), by the Glikson Foundation, by the Minerva Foundation, Munich, Germany, by Contract CT1*CT93-0063 from the Commission of the European Union, and by the Dutch Foundation for Fundamental Research on Matter (FOM).

[1] G. Blatter *et al.*, Rev. Mod. Phys. **66**, 1125 (1994).
[2] D. S. Fisher *et al.*, Phys. Rev. B **43**, 130 (1991).
[3] D. R. Nelson, Phys. Rev. Lett. **60**, 1973 (1988).
[4] L. I. Glazman and A. E. Koshelev, Phys. Rev. B **43**, 2835 (1991); L. L. Daemen *et al.*, Phys. Rev. Lett. **70**, 1167 (1993); Phys. Rev. B **47**, 11 291 (1993).
[5] A. Houghton, R. A. Pelcovits, and A. Sudbo, Phys. Rev. B **40**, 6763 (1989); E. H. Brandt, Phys. Rev. Lett. **63**, 1106 (1989); G. Blatter and B. I. Ivlev, Phys. Rev. B **50**, 10 272 (1994).
[6] G. Blatter, V. B. Geshkenbein, A. I. Larkin, and H. Nordborg (to be published).
[7] H. Safar *et al.*, Phys. Rev. Lett. **69**, 824 (1992); W. K. Kwok *et al.*, Phys. Rev. Lett. **69**, 3370 (1992); W. Jiang *et al.*, Phys. Rev. Lett. **74**, 1438 (1995); S. L. Lee *et al.*, Phys. Rev. Lett. **71**, 3862 (1993); H. Pastoriza *et al.*, Phys. Rev. Lett. **72**, 2951 (1994).
[8] H. Safar *et al.*, Phys. Rev. Lett. **70**, 3800 (1993); D. J. Bishop (private communication).
[9] R. Cubbit *et al.*, Nature (London) **365**, 407 (1993).
[10] E. Zeldov *et al.*, Nature (London) **375**, 373 (1995).
[11] V. N. Kopylov *et al.*, Physica (Amsterdam) **170C**, 291 (1990).
[12] N. Chikumoto *et al.*, Phys. Rev. Lett. **69**, 1260 (1992).
[13] M. Daeumling *et al.*, Nature (London) **346**, 332 (1990).
[14] L. Krusin-Elbaum *et al.*, Phys. Rev. Lett. **69**, 2280 (1992); Y. Yeshurun *et al.*, Phys. Rev. B **49**, 1548 (1994).
[15] G. Yang *et al.*, Phys. Rev. B **48**, 4054 (1993).
[16] T. Tamegai *et al.*, Physica (Amsterdam) **223C**, 33 (1993).
[17] K. Kishio *et al.*, in *Proceedings of the Seventh International Workshop on Critical Currents in Superconductors*, edited by H. W. Weber (World Scientific, Singapore, 1994), p. 339.
[18] N. Motohira *et al.*, J. Ceram. Soc. Jpn. Int. Ed. **97**, 994 (1989).
[19] T. W. Li *et al.*, J. Cryst. Growth **135**, 481 (1994).
[20] T. W. Li *et al.*, Physica (Amsterdam) **224C**, 110 (1994).
[21] T. W. Li *et al.*, Physica (Amsterdam) **257C** (to be published).
[22] J.-Y. Genoud *et al.*, Physica (Amsterdam) **242C**, 143 (1995).
[23] L. Forro, Phys. Lett. A **179**, 140 (1993); Y. Kotaka *et al.*, Physica (Amsterdam) **235C-240C**, 1529 (1994).
[24] E. Zeldov *et al.*, Phys. Rev. Lett. **73**, 1428 (1994).
[25] E. Zeldov *et al.*, Europhys. Lett. **30**, 367 (1995).
[26] D. Majer *et al.*, Physica (Amsterdam) **235C-240C**, 2765 (1994).
[27] C. P. Bean, Phys. Rev. Lett. **8**, 250 (1962).
[28] E. Zeldov *et al.*, Phys. Rev. B **49**, 9802 (1994); E. H. Brandt and M. V. Indenbom, Phys. Rev. B **48**, 12 893 (1993).
[29] R. Sasik and D. Stroud, Phys. Rev. B **52**, 3696 (1995).